Analyst

Accepted Manuscript

ROYAL SOCIETY OF CHEMISTRY

www.rsc.org/analyst

Graphical Abstract:

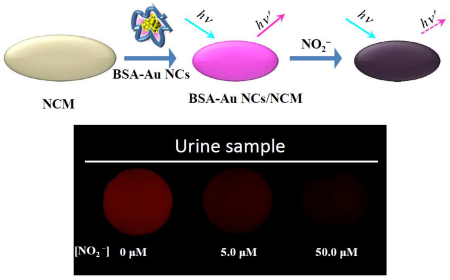

BSA-Au NCs (bovine serum albumin stabilized gold nanoclusters)-modified nitrocellulose membrane (BSA-Au NCs/NCM) has been fabricated for sensing nitrite in urine.

Cite this: DOI: 10.1039/c0xx00000x

www.rsc.org/xxxxxx

PAPER

Nitrite ion-induced fluorescence quenching of luminescent BSA-Au_{25} nanoclusters: mechanism and application

Binesh Unnikrishnan,[a] Shih-Chun Wei,[a] Wei-Jane Chiu,[a] Jinshun Cang,[c] Pang-Hung Hsu,[*,a,b] and Chih-Ching Huang[*,a,b,d]

Received (in XXX, XXX) Xth XXXXXXXXX 20XX, Accepted Xth XXXXXXXXX 20XX

DOI: 10.1039/b000000x

Fluorescence quenching is an interesting phenomenon which is highly useful in developing fluorescence based sensors. A thorough understanding of the fluorescence quenching mechanism is essential to develop efficient sensors. In this work, we investigated different aspects governing the nitrite ion-induced fluorescence quenching of luminescent bovine serum albumin stabilized gold nanoclusters (BSA-Au NCs) and their application for sensing nitrite in urine. The probable events leading to photoluminescence (PL) quenching by nitrite ions were discussed on the basis of the results obtained from ultraviolet-visible (UV-Vis) absorption spectroscopy, X-ray photoelectron spectroscopy (XPS), fluorescence measurements, circular dichroism (CD) spectroscopy, zeta potential and light scattering studies (DLS). These studies suggested that PL quenching mainly occurred through the oxidation of Au(0) atoms to Au(I) atoms in the core of BSA-Au NCs mediated by nitrite ions. The interference caused by certain species such as Hg^{2+}, Cu^{2+}, CN^{-}, S^{2-} glutathione, cysteine , etc. during the nitrite determination by fluorescence quenching were eliminated by using masking agents and optimising the conditions. Based on the findings we proposed a BSA-Au NCs modified membrane based sensor which would be more convenient for the real life application such as detection nitrite in urine samples. BSA-Au NCs-modified nitrocellulose membrane (NCM) enabled the detection of nitrite at a level as low as 100 nM in aqueous solutions. This Au NCs-based paper probe was validated as exhibiting good performance for nitrite analysis in environmental water and urine samples, which renders it useful in practical applications.

1 Introduction

Fluorescent gold nanoclusters (Au NCs) have emerged as an indispensable material for bioimaging,[1,2] biosensing and photonics.[3] owing to their unusual optical and electrical properties.[4–7] Au NCs with the sizes within the range of the Fermi wavelength of electrons show quantum confinement effect and acquire discrete energy levels.[8,9] One of the major factors that controls the stability, size and photoluminescence (PL) properties of these Au NCs in solution is the functional groups which are protecting them, called capping ligands. The most widely used capping ligands for the synthesis of Au NCs are thiol containing molecules.[10,11] The strong interaction between the Au and S atoms enables the formation and stability of NCs with a small number of atoms to hundreds of atoms.[12,13] Recently, synthesis of many protein based Au NCs have been reported.[14–16] Au NCs prepared in the presence of proteins such as bovine serum albumin (BSA) are highly water soluble and stable against aggregation.[15] Furthermore, when compared with semiconductive quantum dots (QDs) and transition metal ion-doped QDs, BSA-Au NCs are more biocompatible and more readily bioconjugated.[17] Owing to their high PL and stability, BSA-Au NCs have been applied in the detection of various analytes, including small molecules (e.g., methotrexate, cysteine, glutathione, vitamin B12, dopamine, quercetin, and glutaraldehyde)[18–24], heavy metal ions (e.g., Cu^{2+}, Hg^{2+}, and Ag^{+}),[25–28] proteins (e.g., cystatin C),[29] and proteases (e.g., trypsin).[30] They have also been employed for cell labelling (e.g., MCF-7)[31] owing to their biocompatibility, ease in preparation, bio-conjugation, and long-wavelength emission.

Among the various Au NCs, BSA-Au NCs with 25 Au atoms has attracted tremendous attention due to its biocompatibility and its suitability for bio-sensing applications by PL quenching. Various inorganic analytes such as CN^{-},[32] S^{2-},[33] NO_2^{-},[34,35] and Hg^{2+},[36] have been detected by PL quenching. Cu^{2+} ions can effectively quench the PL of BSA-Au NCs when it is chelated with glycine in the BSA chain which can be used to detect other species such as Hg^{2+} that can take away Cu^{2+} and restore the PL.[37] The PL quenching of the BSA-Au NCs may occur due to many factors such as aggregation, energy transfer, cyanide-etching, photo-induced electron transfer or change in the oxidation state of Au atoms in the cluster. Therefore, a thorough understanding of PL quenching mechanism will help the design and development of highly selective PL based sensors.

Due to the adverse effects caused by nitrite to human health, the need for nitrite determination in environmental and urine or other biological samples are highly important. For example,

excessive amounts of nitrite typically used for food preservation have been proved to be carcinogenic, teratogenic, or mutagenic because nitrite reacts with amines and results in the formation of N-nitroso compounds.[38–40] Nitrites irreversibly react with oxyhemoglobin to produce methemoglobin in the bloodstream, thereby interfering with oxygen transport in the blood and causing a condition called methemoglobinemia.[41] The nitrite ion is also of interest as a nitric oxide metabolite in numerous physiological processes related to neurotransmission, vasodilatation, inflammation, cell proliferation, and apoptosis.[42] The excessive concentration of nitrite in oceans, rivers, and drinking water has caused serious hazards to human health and aquatic organisms.[43–46] A positive result for nitrite detection in urine indicates a urinary tract infection (gram-negative rods such as *Escherichia coli* (*E. coli*) are more likely to give a positive test). Usually, the bacteria found in urine originate from the digestive tract. The most common organism responsible for urinary tract infections is *E. coli.*[47] Moreover, the detection of nitrite in urine provides evidence of not only bacteriuria but also the presence of leukocytes.[48] However, determination of nitrite in urine and environmental samples by PL quenching method is a challenge due to the presence of some interferrants. For example, Cu^{2+}, Hg^{2+}, S^{2-}, CN^{-}, glutathione, cysteine, etc., might interfere nitrite determination in environmental water and urine samples. Liu *et al*. reported the detection of nitrite in water samples by fluorescence quenching of BSA-Au NCs.[34] However, at these conditions, the possibility of interference due to inorganic ions such as CN^{-}, Hg^{2+}, Cu^{2+} etc, in waters samples is very high, which were not discussed in their report. Similarly, Yue *et al*. reported the detection of nitrite in water samples; however, interference issues due to Hg^{2+} and CN^{-} were not discussed or solved.[35] Moreover, few reports are available for nitrite determination in complicated biological samples such as urine. Hence, an in-depth study of the nitrite-induced quenching mechanism at various conditions and in the presence of common interfering species is necessary to detect nitrite in urine.

In this work, we made a detailed investigation using ultraviolet-visible (UV-Vis) absorption spectroscopy, X-ray photoelectron spectroscopy (XPS), circular dichroism (CD) spectroscopy, zeta potential, and light scattering to understand the various aspects of nitrite induced PL quenching. Based on the studies we suggested the mechanism of PL quenching, optimum conditions and use of masking agents to reduce the interference in real sample analysis.

2 Experimental

2.1 Chemicals and Materials

Bovine serum albumin (BSA), phosphoric acid (H_3PO_4), sodium phosphate (Na_3PO_4), and sodium nitrite ($NaNO_2$) were purchased from Sigma-Aldrich (Milwaukee, WI, USA). Hydrogen tetrachloroaurate(III) trihydrate ($HAuCl_4 \cdot 3H_2O$), sodium cyanide (NaCN), sodium thiocyanate (NaSCN), sodium acetate (CH_3COONa), sodium bromide (NaBr), sodium chloride (NaCl), sodium iodide (NaI), sodium nitrate ($NaNO_3$), sodium sulfide (Na_2S), sodium sulfate (Na_2SO_4), sodium thiosulfate ($Na_2S_2O_3$), mercury(II) chloride ($HgCl_2$), copper(II) chloride ($CuCl_2$), ethylenediamine tetraacetic acid (EDTA), sodium borohydride ($NaBH_4$), glutathione, and cysteine were obtained from Alfa Aesar (Ward Hill, MA, USA). The 100 mM phosphate buffer solution was adjusted to pH 3 by mixing different volume ratios of H_3PO_4 (100 mM) and Na_3PO_4 (100 mM). Nitrocellulose membrane (NCM) was purchased from GE Healthcare Bioscience (Buckinghamshire, UK). Milli-Q ultrapure water (Millipore, Billerica, MA) was used in all the experiments.

2.2 Preparation and characterization of BSA-Au NCs

BSA-Au NCs was prepared by following a previously reported procedure.[15] The BSA was used as such without any denaturing process. In a typical process, 5 mL of aqueous BSA solution (50 mg/mL, 37 ℃) was added to 5 mL of $HAuCl_4$ solution (10 mM, 37 ℃) with vigorous stirring. Approximately 2 min later 0.5 mL of NaOH (1 M) was introduced and the reaction was allowed to proceed at 37 ℃ for 12 h with vigorous stirring. The BSA-protected Au_{25} nanoclusters thus produced were stored at room temperature. The concentration of the as-prepared BSA-Au NCs is calculated as 200 μM.

Circular dichroism (CD) spectroscopy measurements of BSA-Au NCs were carried out using a J-815 spectropolarimeter (JASCO, Inc., Easton, MD). The PL and UV-Vis absorption spectra of BSA-Au NCs were recorded using a microplate spectrophotometer (Synergy 4 Multi-Mode, Biotek Instruments, Winooski, VT). For the analysis using X-ray photoelectron spectroscopy (XPS; PHI 5000 VersaProbe XPS, Ulvac Technologies, Japan) portions of the BSA-Au NC solutions (10 μL) were placed on a Si substrate and then dried at ambient temperature. The XPSPEAK software (Version 4.1) was used to deconvolute narrow-scan XPS spectra of Au 4f of BSA-Au NCs in the absence and presence of nitrite ions using adventitious carbon to calibrate the binding energy of C1s (284.5 eV).

2.3 Nitrite induced PL quenching of BSA-Au NCs

A series of mixtures (0.5 mL) of nitrite ions (0–100 μM) and 0.2 μM BSA-Au NCs in buffer solution (50 mM sodium phosphate; pH 3) were equilibrated at room temperature for 1 h and then transferred separately into 96-well microtiter plates. Their PL spectra were recorded using a Synergy 4 Multi-Mode microplate spectrophotometer with excitation wavelength of 375 nm.

2.4 Fabrication of BSA-Au NCs/NCM for the detection of nitrite ions

Ten pieces of an NCM were cut to a size of 0.3 cm (radius) and immersed in the BSA-Au NC solution (20 μM, 10 mL) in a 20 mL sample bottle. After 3 h of incubation, BSA-Au NC-modified NCM (BSA-Au NCs/NCM) was gently washed with DI water (approximately 20 mL) and then immersed in 0.1% BSA (10 mL) solution for 1 h for blocking the unspecific sites. Subsequently, BSA-Au NCs/NCM was gently washed with DI water (approximately 20 mL) for 30 s and then air-dried at room temperature for 1 h prior to use. The BSA-Au NCs/NCM probes remained stable for at least 3 months when stored at room temperature in the dark. The image of BSA-Au NPs/NCM for PL analysis was obtained using an inverted microscope (IX71, Olympus, NY, USA). Their PL spectra were recorded using a Synergy 4 Multi-Mode microplate spectrophotometer.

3 Results and Discussion

3.1 Nitrite-induced PL quenching of BSA-Au NCs

BSA-Au_{25} nanoclusters were prepared from a mixture of BSA and $AuCl_4^-$ in highly basic conditions (50 mM NaOH).[15] During the synthesis of Au NCs, initially, Au^{3+} ions were mainly reduced by the 21 tyrosine (Tyr) residues in BSA through the phenolic groups in alkaline medium.[15] Clusters composed of 25 gold atoms were formed and stabilized by the thiol group of cysteine in BSA. BSA-Au NCs have been proposed to have a core–shell structure in which 13 Au(0) atoms form an icosahedral core surrounded by six —S−Au(I)−S−Au(I)−S— staples constructed through various Au–Au and Au–S bonds.[49] Quantum yield (QY) of the as-prepared BSA-Au NCs is approximately 6%, as assessed by comparison with quinine (QY, 53%). We compared the PL spectrum that was recorded on the same day of preparation (1st day, denoted as BSA-Au NCs/1st d) and after 7 days (7th day, denoted as BSA-Au NCs/7th d) in the absence and presence of nitrite in a 50 mM phosphate buffer solution (pH 3). After being excited at 375 nm, BSA-Au NCs showed an emission band centered at 660 nm (curve A in Fig. 1), which was consistent with the observation of Xie *et al.*[36] PL of BSA-Au NCs originated from the icosahedral core of Au(0) atoms mixed with [–S–Au(I)–S–Au(I)–S–] semirings.[49] The electron–phonon scattering, Au(I)–Au(I) interaction, and exterior ligands play major roles in PL intensity and stability.[49] BSA-Au NCs/7th d (curve B in Fig. 1) showed a slight increase in PL intensity (approximately 15%) compared with BSA-Au NCs/1st d. This could be due to small conformational changes of BSA. This fact is supported by a recent report by Zhang *et al*. which shows that the conformational changes of the ligand enhances the PL for BSA protected Au NCs.[50] Moreover, the PL quenching effect on BSA-Au NCs/7th d (approximately 42.0% of its original value) by nitrite ions (10 μM) was much higher than that of BSA-Au NCs/1st d (approximately 27.2%). In contrast, BSA-Au NCs did not show significant changes in their UV-visible absorption peak in the presence of nitrite (Fig. S1, Supporting Information†) suggesting that nitrite did not induce aggregation of BSA-Au NCs or significant structural changes in BSA. The insignificant difference between the fluorescence lifetimes of the BSA-Au NCs/7th d in the absence and presence of 10 μM nitrite (Fig. S2, Supporting Information) suggested a static quenching mode for the NO_2^- induced fluorescence quenching of BSA-Au NCs.[35] The PL quenching of BSA-Au NCs/7th d reached its maximum within 30 min after nitrite (10 μM) was added to the mixture (Inset, Fig. 1).

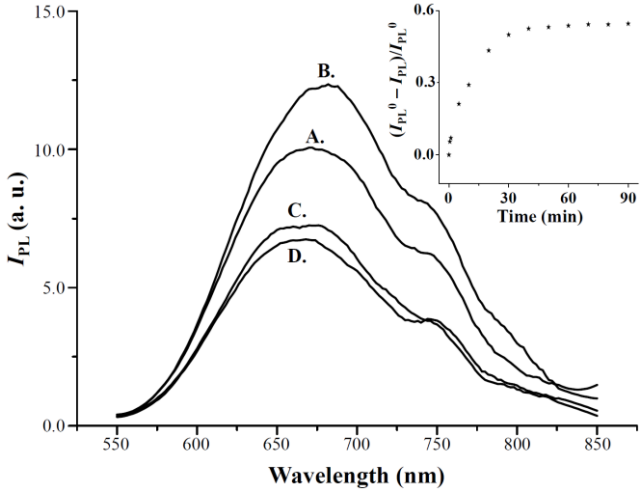

Fig. 1. PL spectra of 50 mM sodium phosphate (pH 3) containing (A, C) BSA-Au NCs/1st d (0.2 μM) and (B, D) BSA-Au NCs/7th d (0.2 μM) in the (A, B) absence and (C, D) presence of nitrite (10 μM). Inset: time course of the relative PL intensity $[(I_{PL}^0 - I_{PL})/I_{PL}^0]$ of BSA-Au NCs/7th d at 660 nm after the addition of nitrite, where I_{PL}^0 and I_{PL} are the PL intensities of BSA-Au NCs/7th d in the absence and presence of nitrite, respectively. Excitation wavelength, 375 nm. PL intensities (I_{PL}) are plotted in arbitrary units (a. u.).

3.1.1 Characterization of BSA-Au NCs by DLS and CD spectroscopy

The significant nitrite-induced PL quenching of BSA-Au NCs/7th d was probably due to its loose BSA structure, which facilitated the interaction of the nitrite ion with the Au cluster. The as-prepared BSA-Au NCs incubated in alkaline solution (pH approximately 12) for 7 days may have undergone some manner of partial denaturation of BSA molecules. The change in the structure of BSA in BSA-Au NCs/7th d may explain the increase in the PL intensity and the enhanced quenching effect of the nitrite anion. Based on dynamic light scattering (DLS) measurements, we estimated the hydrodynamic diameters of BSA-Au NCs/1st d (2 μM) and BSA-Au NCs/7th d (2 μM) assemblies as being 10.1 (±0.6; n =5) and 12.1 (±1.5; n = 5) nm, respectively, supporting that BSA underwent only a slight change (denaturation) after 7 days of incubation. At pH above 9, BSA undergoes changes in conformation and attains the basic B form and after 3 or 4 days it will be changed to A form by an isomerisation process[51] which provides an appropriate milieu for Au NPs inside the BSA.

The CD spectra of BSA-Au NCs/1st d and BSA-Au NCs/7th d are shown in Fig. 2. The CD spectrum of BSA exhibited two negative minima in the ultraviolet region at 210 and 222 nm, which were characteristic of an α-helical protein structure. However, after the formation of BSA-Au NCs, the CD spectra showed that the negative band observed at 210 nm for BSA shifted to 208 nm. Moreover, the valley of BSA-Au NCs/7th d at 222 nm was much and slight shallower than that of pure BSA and BSA-Au NCs/1st d, respectively. This observation implies a decrease in the α-helical content and an increase in random coil

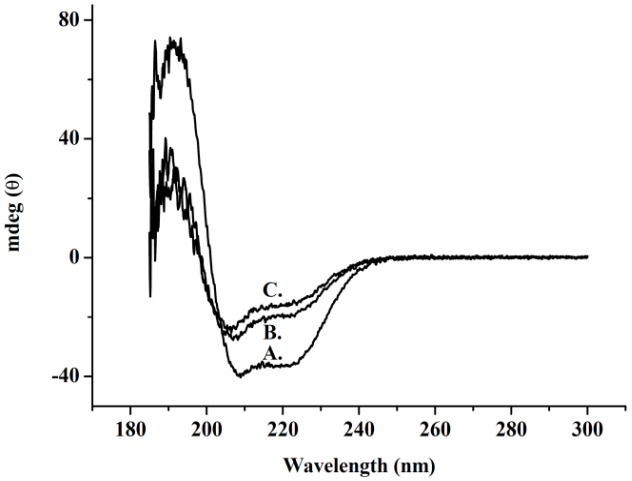

Fig. 2 CD spectra of 50 mM sodium phosphate containing (A) BSA, (B) BSA-Au NCs/1st d (2 μM) and (C) BSA-Au NCs/7th d (2 μM). Other conditions were the same as those described in Fig. 1.

structures of BSA-Au NCs/7thd.

3.1.2 Study of nitrite-induced quenching by zeta potential, light scattering and XPS techniques

To understand the nitrite-induced PL quenching of BSA-Au NCs/7thd, we performed zeta potential, light scattering, and XPS measurements. The zeta potentials of BSA-Au NCs/7thd in the absence and presence of 10 μM nitrite were 4.94 ± 0.31 mV (n = 5) and 4.88 ± 0.25 mV (n = 5), respectively, in 50 mM sodium phosphate (pH 3). We also determined the intensities of the static light scattering of BSA-Au NCs/7thd (2 μM) in the absence and presence of nitrite (100 μM) as being 33.4 ± 4.3 kcps (n = 5) and 34.4 ± 2.8 kcps (n = 5), respectively. The zeta potentials and static light scattering results suggest that the possibility of PL quenching due to nitrite-induced changes in particle size, surface charge and aggregation can be ruled out. The binding energy (BE) for the Au 4f$_{7/2}$ electrons in BSA-Au NCs/7thd in the absence of nitrite was 84.1 eV (curve A, Fig. 3), which was within the range from 83.5 eV for bulk Au to 85.0 eV for a polynuclear Au(I)–thiol complex.[52] In contrast, BE for the Au 4f$_{7/2}$ electrons in BSA-Au NCs/7thd in the presence of 100 μM nitrite was 84.9 eV (curve B, Fig. 3), suggesting an increase in the oxidation state of the Au atoms in Au NCs. Because PL intensity was dramatically influenced by the polynuclear Au(I)–thiol units on the surface,[15] the nitrite-induced PL quenching presumably occurred mainly through the oxidation of Au(0) atoms to Au(I) in the core of BSA-Au NCs mediated by the nitrite ions through electron transfer between the nitrite and Au(0) units in an acidic solution. In acidic medium, nitrite anions react with H^+ ions to form nitrous acid, which further reacts with H^+ ions to form nitrosyl cations (NO^+) and water, as shown in equation (1).[53]

$$^{-}O\text{–}N{=}O \xrightarrow{H^+} HO\text{–}N{=}O \xrightarrow{H^+} \underset{\underset{H^+}{|}}{HO\text{–}N{=}O} \xrightarrow{H^+} N{\equiv}O^+ + H_2O \quad \text{---(1)}$$

The nitrosyl cation is electron deficient and can react with Au NCs in acidic medium through electron transfer process. In addition, in acidic medium, the nitrite ion is a strong oxidizer (2 HNO_2 + 4 H^+ + 4 e^- ↔ N_2O + 3 H_2O; E^0 = 1.29V);[54] therefore, it could direct the oxidation of BSA-Au NCs. Because nitrite in an acidic solution is unstable with respect to the disproportionation reaction (3 $HNO_{2(aq)}$ ↔ H_3O^+ + NO_3^- + 2 NO),[55] we cannot rule out the possibility of NO-induced PL quenching of BSA-Au NCs occurring through the S-nitrosylation reaction between NO and cysteine to form S-nitrosothiol.[56]

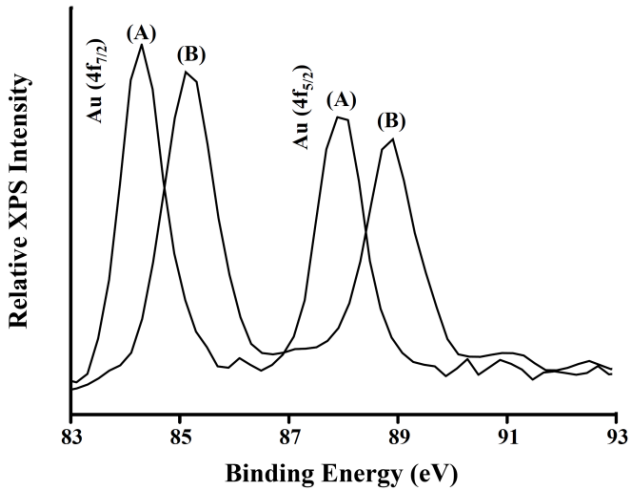

Fig. 3 Au 4f core-level photoelectron spectra of BSA-Au NCs/7thd (2 μM) in the (A) absence and (B) presence of nitrite (100 μM). The binding energy (BE, 285.3 eV) of the alkyl chain C 1s orbital is given as an internal reference.

3.2 Application of BSA-Au NCs for detection of nitrite

3.2.1 Effect of pH on selectivity and sensitivity

We further studied the effect of pH on the selectivity and sensitivity of the BSA-Au NCs/7thd probe for the detection of nitrite. We determined the relative PL intensity decrease of BSA-Au NCs/7thd (0.2 μM) at 650 nm [(I_{PL}^0 − I_{PL})/I_{PL}] in the presence of 22 different anions and metal ions species (10 μM) in sodium phosphate (50 mM) at pH 3, pH 7, and pH 11. Fig. 4A reveals that the BSA-Au NCs/7thd probe in sodium phosphate at pH 3 exhibited superior selectivity compared with that observed at pH 7 and pH 11. In a neutral or basic medium, the basic forms of S^{2-}, CN^-, cysteine, and glutathione react with BSA-Au NCs through strong Au–S, Au–CN, or Au–thiol interactions. Fortunately, a greater selectivity of the BSA-Au NCs/7thd probe toward nitrite ions was readily achieved in an acidic medium (50 mM sodium phosphate, pH 3). However, strong PL quenching of BSA-Au NCs was observed in the presence of Cu^{2+} or Hg^{2+} through strong Cu–Au and Hg–Au aurophilic attractions. In the presence of the masking agents ethylenediamine tetraacetic acid (EDTA; 1.0 mM) and $NaBH_4$ (0.5 mM), the BSA-Au NCs/7thd sensor behaved almost completely free of interference from Cu^{2+} and Hg^{2+}, respectively. EDTA, a popular ligand for most cations [formation constant, logK (Cu^{2+}–EDTA) = 18.80], was useful in providing more competitive binding and better PL recovery. Hg^{2+} also strongly bound EDTA [logK (Hg^{2+}–EDTA) = 21.7]; however, the complexation did not change the oxidation state of mercury, and it was still capable of binding Au^+ for quenching.[36] Borohydride ($NaBH_4$ + $8OH^-$ → $NaBO_2$ + $6H_2O$ + $8e^-$) can easily reduce the Hg^{2+} [E°(Hg^{2+}/Hg) = 0.85 V] but not the more stable Cu^{2+} [E°(Cu^{2+}/Cu) = 0.34 V] or [E°(Cu^{2+}/Cu^+) = 0.17 V]. As indicated in Fig. 4B, BSA-Au NCs/7thd showed greater sensitivity for the detection of nitrite anions at pH 3 (50 mM sodium phosphate) owing to the high oxidizability of nitrite only in an acidic environment. The high oxidizability of nitrite only under acidic conditions is also very helpful to distinguish it from other oxidants in the same system. BSA undergoes conformational changes with the change in pH. For example, according to Leonard *et al.* BSA undergoes an abrupt expansion at pH 4.3 and will attain E conformation in the pH range from 2.8 to 3.4 that could be another reason why nitrite induced PL quenching of BSA-Au NCs is maximum in pH 3.[57] Stobiecka *et al.* also reported a reversible conformational transition for BSA film on gold piezoelectrode due to the change in the electrode charge and local pH caused by the electrocatalytic nitrate ion reduction.[58] The plots of [(I_{PL}^0 − I_{PL})/I_{PL}] against the logarithms of the concentrations of nitrite over the range from 100 nM to 100 μM were all linear, with correlation coefficients (R) of 0.97 (Fig. 4Ba). I_{PL}^0 and I_{PL} are the PL intensity of the BSA-Au NCs/7thd probe in the absence and presence of nitrite, respectively. This probe enables analyses of nitrite with a limit of detection (LOD at S/N = 3) of 50 nM, which is considerably lower than the

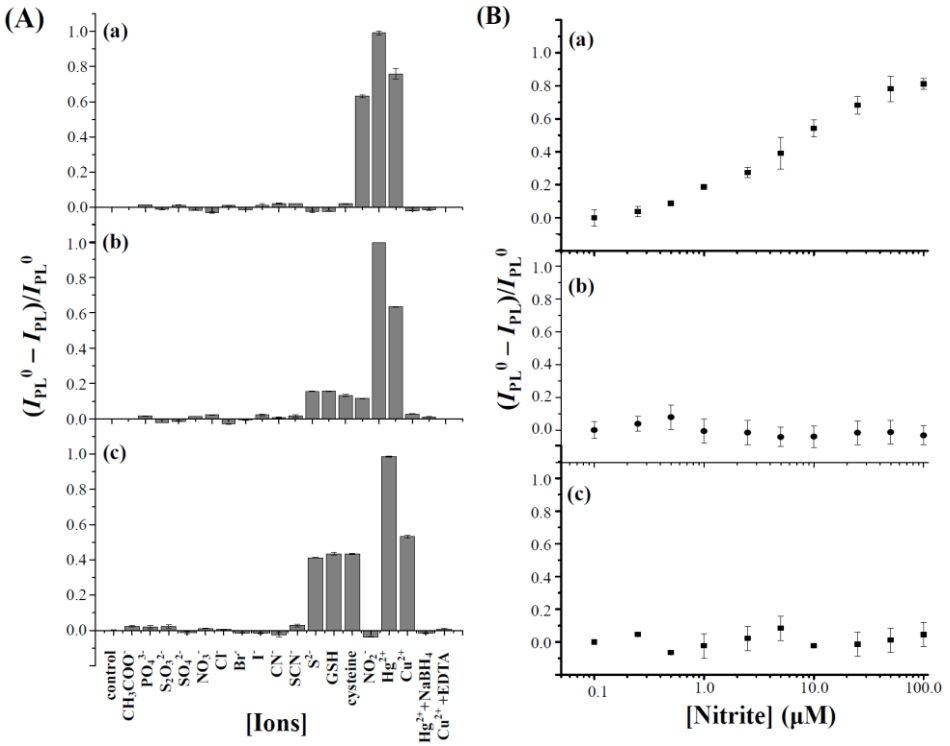

Fig. 4 (A) Relative PL changes $[(I_{PL}^0 - I_{PL})/I_{PL}^0]$ in the BSA-Au NCs/7thd (0.2 μM) probe toward nitrite (10 μM), other anions (10 μM each), cysteine (10 μM), glutathione (10 μM), and heavy metal ions (10 μM each) in 50 mM sodium phosphate at (a) pH 3, (b) pH 7, and (c) pH 11. (B) Relative PL intensities $[(I_{PL}^0 - I_{PL})/I_{PL}^0]$ of BSA-Au NCs/7thd (0.2 μM) plotted with respect to the nitrite concentration (0–100 μM) in 50 mM sodium phosphate at (a) pH 3, (b) pH 7, and (c) pH 11. The concentrations of $NaBH_4$ and EDTA masking agents for Hg^{2+} and Cu^{2+} are 0.5 mM and 1.0 mM, respectively. Error bars represent standard deviations from three repeated experiments. Other conditions were the same as those described in Fig. 1.

maximum level of nitrite in drinking water (approximately 21.7 μM) permitted by the U.S. Environmental Protection Agency (EPA).[59,60] This LOD was comparable with or better than those obtained using other nanomaterial-based sensors for nitrite.[61–66] The good sensitivity and wide linearity for the detection of nitrite suggests a great potential of BSA-Au NCs/7thd for application in bioassays.

3.2.2 BSA-Au NCs/NCM-based sensor for nitrite

We further developed a simple paper-based BSA-Au NCs/NCM nanocomposite for nitrite sensing. The BSA-Au NCs/NCM film was prepared for the luminescent detection of nitrite by taking advantage of the easy immobilization of BSA-Au NCs into NCM and the strong quenching ability of nitrite toward BSA-Au NCs. NCMs are widely used as blotting matrices for protein immobilization, with hydrophobic interactions being mainly responsible for the adsorption of proteins onto NCM, allowing impurities to be removed through washing. The PL images of BSA-Au NCs/NCM shown in Fig. 5 reveal that the NC fibers were homogenously associated with the adsorbed BSA-Au NCs. We also used BSA-Au NCs/NCM for nitrite sensing. We recorded the red PL component (I_{PL}) of BSA-Au NCs after reaction with nitrite (0–100 μM). In the presence of solutions of 50 mM sodium phosphate (pH 3), BSA-Au NCs/NCM detected nitrite at a level as low as 100 nM. To validate the practicality of our proposed sensing strategy for analysis of environmental samples, we used BSA-Au NCs/NCM to determine the concentrations of nitrite spiked in tap, river, lake, and sea water samples. Prior to analysis, the samples were filtered through a 0.2-μm membrane and diluted twofold in a 50 mM sodium phosphate solution (pH 3). The concentrations of nitrite spiked in twofold-diluted tap, river, lake, and sea water samples in the 0–100 μM range were detected using the BSA-Au NCs/NCM probe. We obtained a similar LOD (100 nM) of nitrite for these four water samples (Fig. S3, Supporting Information†). The sensing parameters of the proposed sensor have been compared with those of other nanomaterial based fluorometric/colorimetric

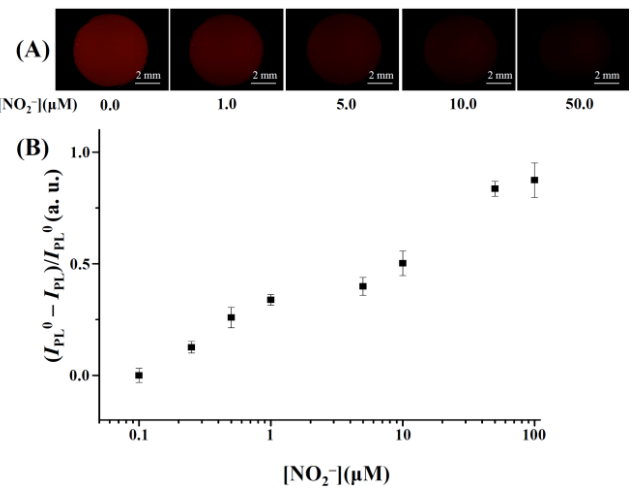

Fig. 5 (A) Photographic images of PL. (B) Relative signal intensities $[(I_{PL}^0 - I_{PL})/I_{PL}^0]$ of BSA-Au NCs/NCM in the presence of nitrite (0–100 μM) in 50 mM sodium phosphate solutions (pH 3). I_{PL}^0 and I_{PL} are the red PL component of BSA-Au NCs/NCM in the absence and presence of nitrite, respectively. Error bars represent standard deviations from four repeated experiments.

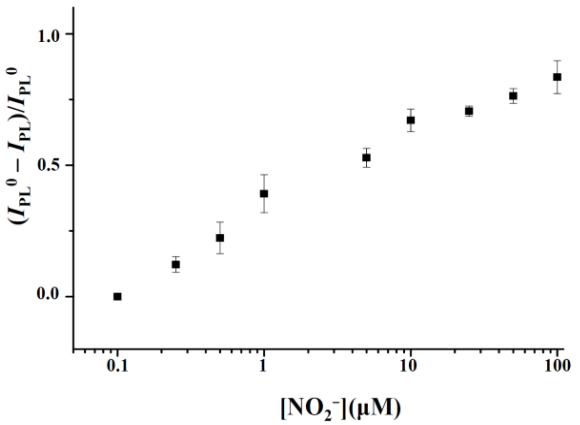

Fig. 6 Relative signal intensities $[(I_{PL}^0 - I_{PL})/I_{PL}^0]$ of BSA-Au NCs/NCM in the presence of spiked nitrite (0–100 μM) in 10-fold-diluted urine samples. Error bars in represent standard deviations from three repeated experiments. Other conditions were the same as those described in Fig. 5.

nitrite sensors (Table S1, Supporting Information). Yue *et al*. detected nitrite in the same linear range and a LOD of 30 nM.[35] However, the study on interference due to Hg^{2+} is lacking, which is essential for real water sample analysis, because Hg^{2+} can quench the fluorescence of BSA-Au NCs by metallophilic Hg^{2+}–Au^+ interaction. Also, CN^- can quench the fluorescence in higher pH by cyanide etching-induced fluorescence quenching of gold nanoclusters.[32] By operating our probe in low pH, such interference was ruled out. Similarly, Liu *et al*. reported a very low detection limit of 1 nM for detection of nitrite in water samples, at pH 7.4, but Hg^{2+}, CN^- inference is not mentioned.[34]

Furthermore, we used our BSA-Au NCs/NCM sensor system to determine nitrite concentrations in human urine samples because their levels can be indicative of bacterial infection. As shown in Fig. 6, the relative signal intensities of $[(I_{PL}^0 - I_{PL})/I_{PL}^0]$ increased on increasing the spiked concentration of nitrite ions in 10-fold-diluted urine samples over the range of 0–100 μM. I_{PL}^0 and I_{PL} are the red PL components of BSA-Au NCs/NCM in the absence and presence of spiked nitrite, respectively. LOD for this complicated biological sample was approximately 250 nM, which is at least one order of magnitude lower than those of other clinical urinary nitrite tests.[67–70] Thus, BSA-Au NCs/NCM system is a practical tool for monitoring nitrite ions in natural water and has a high potential for the diagnosis of urinary tract infections.

Conclusions

A detailed investigation was carried out on the various factors influencing nitrite-induced PL quenching of BSA-Au NCs using different techniques. BSA-Au NCs went through some conformational changes after seven days of preparation, notably, a decrease in the α-helical content and an increase in the random coil structure, and it resulted in increase in PL. However, nitrite ion did not make any major structural changes to BSA. Among the various possible quenching mechanisms, nitrite induced quenching by the oxidation of Au(0) to Au(I) was the dominant one. The optimum condition for the effective determination of nitrite without interference was found to be pH 3. Also, different factors that interfere the nitrite quantification in environmental and urine samples have been studied. Based on the findings about the mechanism of PL quenching, influence of pH and interference studies, we proposed a BSA-Au NCs modified NCM based nitrite sensor. The sensor can be used as a strip, and it successfully overcome the interference of heavy metals such as Cu^{2+} and Hg^{2+} and other common interferrents such as CN^-, S^{2-}, glutathione, cysteine, etc. in water as well as urine samples.

Acknowledgement

This study was supported by the National Science Council of Taiwan under contract NSC 101-2628-M-019-001-MY3.

Notes and references

[a]*Institute of Bioscience and Biotechnology, National Taiwan Ocean University, 20224, Keelung, Taiwan. E-mail: phsu@ntou.edu.tw; Fax: 011-886-2-2462-2320; Tel: 011-886-2-2462-2192 ext. 5567*
[b]*Institute of Bioscience and Biotechnology, Center of Excellence for the Oceans, National Taiwan Ocean University, 20224, Keelung, Taiwan. E-mail: huanging@ntou.edu.tw; Fax: 011-886-2-2462-2320; Tel: 011-886-2-2462-2192 ext. 5517*
[c]*Department of Chemistry, Yancheng Institute of Industry Technology, Jiangsu, 224005, P. R. China*
[d]*School of Pharmacy, College of Pharmacy, Kaohsiung Medical University, Kaohsiung 80708, Taiwan*

†Electronic Supplementary Information (ESI) available: UV-visible spectra, fluorescence decay and real sample analysis results are presented in Fig. S1–S3 and a comparison of parameters of nitrite sensors is given in Table S1. See DOI: 10.1039/b000000x/

1 L. Shang and G. U. Nienhaus, *Biophys. Rev.*, 2012, **4**, 313–322.
2 S. Palmal and N. R. Jana, *WIREs Nanomed Nanobiotechnol.*, 2013, doi: 10.1002/wnan.1245.
3 D. M. Chevrier, A. Chatt and P. Zhang, *J. Nanophoton*., 2012, **6**, 064504-1–064504-16.
4 R. Jin, *Nanoscale*, 2010, **2**, 343−362.
5 J. F. Parker, C. A. Fields-Zinna, and R. W. Murray, *Acc. Chem. Res.*, 2010, **43**, 1289–1296.
6 X. Wu, X. He, K. Wang, C. Xie, B. Zhou and Z. Qing, *Nanoscale*, 2010, **2**, 2244–2249.
7 L. Shang, N. Azadfar, F. Stockmar, W. Send, V. Trouillet, M. Bruns, D. Gerthsen and G. U. Nienhaus, *Small*, 2011,**7**, 2614–2620.
8 H. Qian, M. Zhu, Z. Wu and R. Jin, *Accounts Chem. Res.*, 2012, **45**, 1470–1479.
9 N. Nishida, E. S. Shibu, H. Yao, T. Oonishi, K. Kimura and T. Pradeep, *Adv. Mater.*, 2008, **20**, 4719−4723.
10 Z. Wu and R. Jin, *Nanolett.*, 2010, **10**, 2568–2573.
11 H.-Y. Chang, H.-T. Chang, Y.-L. Hung, T.-M. Hsiung, Y.-W. Lin and C.-C. Huang, *RSC Advances*, 2013, **3**, 4588–4597.
12 D. Jiang, *Nanoscale*, 2013, **5**, 7149 – 7160.
13 J. Zheng, C. Zhou, M. Yu and J. Liu, *Nanoscale*, 2012, **4**, 4073–4083.
14 Y. Wang, J. Chen and J. Irudayaraj, *ACS Nano*, 2011, **5**, 9718–9725.
15 J. Xie, Y. Zheng and J. Y. Ying, *J. Am. Chem. Soc.*, 2009, **131**, 888–889.
16 H. Wei, Z. Wang, L. Yang, S. Tian, C. Hou and Y. Lu, Analyst, 2010, **135**, 1406–1410.
17 L. Shang, S. Dong, and G. U. Nienhaus, *Nano Today*, 2011, **6**, 401–418.
18 Z. Chen, S. Qian, J. Chen, X. Chen, W. Gao and Y. Lin, *J. Nanopart. Res.*, 2012, **14**, 1264–1272.
19 M.-L. Cui, J-M. Liu, X.-X. Wang, L.-P. Lin, L. Jiao, L.H. Zhang, Z.-Y. Zheng and S.-Q. Lin, *Analyst*, 2012, **137**, 5346–5351.
20 D. Tian, Z. Qian, Y. Xia and C. Zhu, *Langmuir*, 2012, **28**, 3945–3951.
21 F. Samari, B. Hemmateenejad, Z. Rezaei and M. Shamsipur, *Anal. Methods*, 2012, **4**, 4155–4160.
22 Y. Tao, Y. Lin, J. Ren and X. Qu, *Biosens. Bioelectron.*, 2013, **42**, 41–46.
23 Z. Chen, S. Qian,J. Chen and X. Chen, *Analyst*, 2012, **137**, 4356–4361.

24 X. Wang, P. Wu, Y. Lv and X. Hou, *Microchem. J.*, 2011, **99**, 327–331.
25 L. Su, T. Shu, Z. Wang, J. Cheng, F. Xue, C. Li and X. Zhang, 2013, *Biosens. Bioelectron.*, **44**, 16–20.
26 Y. Cai, L. Yan, G. Liu, H. Yuan and D. Xiao, *Biosens. Bioelectron.*, 2013, **41**, 875–879.
27 D. Cao, J. Fan, J. Qiu, Y. Tu and J. Yan, 2013, *Biosens. Bioelectron.*, **42**, 47–50.
28 Y. Yue, T. -Y. Liu, H. -W. Li, Z. Liu and Y. Wu, *Nanoscale*, 2012, **4**, 2251–2254.
29 H. Lin, L. Li, C. Lei, X. Xu, Z. Nie, M. Guo, Y. Huang and S. Yao, *Biosens. Bioelectron.*, 2013, **41**, 256–261.
30 L. Hu, S. Han, S. Parveen, Y. Yuan, L. Zhang and G. Xu, *Biosens. Bioelectron.*, 2012. **32**, 297–299.
31 A. Retnakumari, S. Setua, D. Menon, P. Ravindran, H. Muhammed, T. Pradeep, S. Nair and M. Koyakutty, *Nanotechnology*, 2010, **21**, 055103.
32 Y. Liu, K. Ai, X. Cheng, L. Huo, and L. Lu, *Adv. Funct. Mater.* 2010, **20**, 951–956.
33 M.-L. Cui, J.-M. Liu, X.-X. Wang, L.-P. Lin, L. Jiao, Z.- Y. Zheng, L.-H. Zhang and S.-L. Jiang, *Sens. Actuators, B*, 2013, **188**, 53–58.
34 H. Y. Liu, G. H. Yang, E. S. Abdel-Halim and J.-J. Zhu, *Talanta*, 2013, **104**, 135–139.
35 Q. L. Yue, L. J. Sun, T. F. Shen, X. H. Gu, S. Q. Zhang and J. F. Liu, *J. Fluoresc.*, 2013, **23**, 1313–1318.
36 J. P. Xie, Y. G. Zheng and J. Y. Ying, *Chem. Commun.*, 2010, **46**, 961–963.
37 J.-M. Liu, M.-L. Cui, S.-L. Jiang, X.-X. Wang, L.-P. Lin, L.-Jiao, L.-H. Zhang and Z.-Y. Zheng, *Anal. Methods*, 2013, **5**, 3942–3947.
38 R. Walker, *Food Addit. Contam. Part A*, 1990, **7**, 717–768.
39 S. A. Kyrtopoulos, *Cancer Surv.*, 1989, **8**, 423–442.
40 S. Odashima, *Oncology*, 1980, **34**, 282–286.
41 T. Y. Chan, *Southeast Asian J Trop Med Public Health*, 1996, **27**, 189–192.
42 E. E. Van Faassen, S. Bahrami, M. Feelisch, N. Hogg, M. Kelm, D. B. Kim-Shapiro, A. V. Kozlov, H. Li, J. O. Lundberg, R. Mason, H. Nohl, T. Rassaf, A. Samouilov, A. Slama-Schwok, S. Shiva, A. F. Vanin, E. Weitzberg, J. Zweier and M. T. Gladwin, *Med. Res. Rev.*, 2009, **29**, 683–741.
43 Y.-T. Hung, E. Butler, C. Y. Kuo and R. Y.-L. Yeh, *Water Environ. Res.*, 2010, **82**, 1448–1467.
44 J. A. Camargo and Á. Alonso, *Environ. Int.*, 2006, **32**, 831–849.
45 A. Cockburn, G. Brambilla, M.-L. Fernández, D. Arcella, L. R. Bordajandi, B. Cottrill, C. Van Peteghem and J.-L. Dorne, *Toxicol. Appl. Pharmacol.*, 2013, **270**, 209–217.
46 C. S. Bruning-Fann and J. B. Kaneene, *Vet. Hum. Toxicol.*, 1993, **35**, 521–538.
47 S. Nys, T. Van Merode, A. I. M. Bartelds and E. E. Stobberingh, *J. Antimicrob. Chemother.*, 2006, **57**, 955–958.
48 M. O. Nava, N. Mirzaei, V. Ebrahimian, M. Molaei, F. Tohidnia and M. Pursafar, *Biomed. Pharmacol. J.*, 2012, **5**, 257–260.
49 X. Wen, P. Yu, Y.-R. Toh and J. Tang, *J. Phys. Chem. C*, 2012, **116**, 11830−11836.
50 M. Zhang, Y. Q. Dang, T. Y. Liu, H. W. Li, Y. Wu, Q. Li, K. Wang and B. Zou, *J. Phys. Chem. C*, 2013, **117**, 639−647.
51 R. A. Curvale, *J. Argent. Chem. Soc.*, 2009, **97**, 174–180.
52 C. Zhou, C. Sun, M. Yu, Y. Qin, J. Wang, M. Kim and J. Zheng, *J. Phys. Chem. C*, 2010, **114**, 7727–7732.
53 S. Ozawa, E. Sakamoto, T. Ichikawa, Y. Watanabe and I. Morishima, *Inorg. Chem.*, 1995, **34**, 6362–6370.
54 Y. Wang, E. Laborda and R. G. Compton, *J. Electroanal. Chem.*, 2012, **670**, 56–61.
55 X. Xing and D. A. Sherson, *Anal. Chem.*, 1988, **60**, 1468–1472.
56 M. Kashiba-Iwatsuki, M. Miyamoto and M. Inoue, *Arch. Biochem. Biophys.*, 1997, **345**, 237–242.
57 W. J. Leonard and J. F. Foster, *J. Biol. Chem.*, 1961, **236**, 2662–2669.
58 M. Stobiecka, M. Hepel and J. Radecki, *Electrochim. Acta*, 2005, **50**, 4873–4887.
59 EPA 816-F-09-004: National Primary Drinking Water Regulations 2009, U.S. Environmental Protection Agency: Washington, D. C., 2009.
60 T. T. Mensinga, G. J. A. Speijers and J. Meulenbelt, *Toxicol. Rev.*, 2003, **22**, 41–51.
61 J. Li, Q. Li, C. Lu and L. Zhao, *Analyst*, 2011, **136**, 2379–2384.
62 Z. Lin, W. Xue, H. Chen and J. –M. Lin, *Anal. Chem.*, 2011, **83**, 8245–8251.
63 P. Wang, Z. Mai, Z. Dai, Y. Li and X. Zou, *Biosens. Bioelectron.*, 2009, **24**, 3242–3247.
64 S. Yang, X. Zeng, X. Liu, W. Wei, S. Luo, Y. Liu and Y. Liu, *J. Electroanal. Chem.*, 2010, **639**, 181–186.
65 M. Muchindu, T. Waryo, O. Arotiba, E. Kazimierska, A. Morrin, A. J. Killard, M. R. Smyth, N. Jahed, B. Kgarebe, P. G. L. Baker and E. I. Iwuoha, *Electrochim. Acta*, 2010, **14**, 4274–4280.
66 S. Yang, X. Liu, X. Zeng, B. Xia, J. Gu, S. Luo, N. Maia and W. Wei, *Sens. Actuators, B*, 2010, **145**, 762–768.
67 H. Semeniuk and D. Church, *J. Clin. Microbiol.*, 1999, **37**, 3051–3052.
68 M. M. Buzayan and R. S. Tobgi, *J. Bahrain Med. Soc.*, 2008, **20**, 124–127.
69 R. L. Christensen, F. M. Creekmore, M. B. Strong and R. A. Lugo, *Hosp. Pharm.*, 2007, **42**, 52–56.
70 R. D. Wammanda, H. A. Aikhionbare and W. N. Ogala, *WAJM*, 2000, **19**, 206–208.